HHS Public Access

Author manuscript

Chem Res Toxicol. Author manuscript; available in PMC 2015 June 04.

Published in final edited form as:

Chem Res Toxicol. 2007 July ; 20(7): 1053–1060. doi:10.1021/tx700101d.

Detection, Characterization, and Decay Kinetics of ROS and Thiyl Adducts of Mito-DEPMPO Spin Trap

Micaël Hardy[†,‡], **Antal Rockenbauer**[§], **Jeannette Vásquez-Vivar**[†,‡], **Christopher Felix**[†], **Marcos Lopez**[†,‡], **Satish Srinivasan**[‖], **Narayan Avadhani**[‖], **Paul Tordo**[⊥], and **B. Kalyanaraman**[†,‡,*]

Department of Biophysics, Medical College of Wisconsin, Milwaukee, Wisconsin 53226, Free Radical Research Center, Medical College of Wisconsin, Milwaukee, Wisconsin 53226, Chemical Research Center, Institute for Structural Chemistry, H-1525 Budapest, P.O. Box 17, Hungary, Department of Animal Biology, School of Veterinary Medicine, University of Pennsylvania, Philadelphia, Pennsylvania, and Laboratoire SREP, UMR 6517 CNRS et Universités d'Aix-Marseille 1, 2 et 3, Centre de Saint Jérôme, 13397 Marseille Cedex 20, France

Abstract

We report here the detection and characterization of spin adducts formed from the trapping of reactive oxygen species (superoxide and hydroxyl radicals) and glutathiyl and carbon-centered radicals by a newly synthesized nitrone, Mito-DEPMPO. This is a cationic nitrone spin trap with a triphenyl phosphonium cation conjugated to the DEPMPO analogue. The Mito-DEPMPO-OOH adduct, formed from the trapping of superoxide by Mito-DEPMPO, was enzymatically generated using xanthine/xanthine oxidase and neuronal nitric oxide synthase, and chemically generated by KO_2 in 18-crown-6. The Mito-DEPMPO-OOH adduct exhibits an eight-line EPR spectrum with partial asymmetry arising from the alternate line-width effect. The half-life of the Mito-DEPMPO-OOH adduct is 2–2.5-times greater than that of the DEPMPO-OOH. The Mito-DEPMPO-SG adduct, formed from the trapping of glutathiyl radicals by Mito-DEPMPO, is 3-times more persistent than the analogue DEPMPO-SG adduct. In this study, we describe the EPR characterization of spin adducts formed from Mito-DEPMPO. The EPR parameters of Mito-DEPMPO adducts are distinctly different and highly characteristic. The detection of superoxide from an intact mitochondrion was feasible with Mito-DEPMPO but not with DEPMPO. We conclude that Mito-DEPMPO nitrone and its analogues are more effective than most nitrone spin traps for trapping superoxide, hydroxyl, and thiyl radicals formed in biological systems, including mitochondria.

[*]To whom correspondence should be addressed. Phone: 414-456-4129. Fax: 414-456-6512. balarama@mcw.edu.
[†]Department of Biophysics, Medical College of Wisconsin.
[‡]Free Radical Research Center, Medical College of Wisconsin.
[§]Institute for Structural Chemistry.
[‖]University of Pennsylvania.
[⊥]UMR 6517 CNRS et Universités d'Aix-Marseille 1, 2 et 3.

Supporting Information Available: Spin trapping of ROS with Mito-DEPMPO, kinetic of the decay of the Mito-DEPMPO and the DEPMPO spin adducts, and the effect of Mito-DEPMPO and DEPMPO on mitochondrial oxygen consumption. This material is available free of charge via the Internet at http://pubs.acs.org.

Introduction

The electron paramagnetic resonance (EPR)-spin trapping technique is the most unambiguous analytical method for detecting and characterizing reactive oxygen species (ROS) and thiyl radicals (RS•) in biological systems (1–8). 5,5-Dimethyl-pyrroline *N*-oxide (DMPO[1]) **1** has remained the spin trap of choice for many years (8–10) despite its limitation. In order to improve superoxide detection, several new nitrone traps, DEP-MPO **2**, EMPO **3**, and BMPO **4**, have been synthesized (11–16) (Figure 1). Superoxide adducts formed from these nitrones are persistent, and their EPR spectra are highly characteristic (8–10). Of these traps, DEPMPO **2** is the most reliable spin trap for detecting the superoxide radical in biological systems because of the persistence of its spin adducts (e.g., DEPMPO-OOH; $t_{1/2}$ = 17 min). However, radical addition on the prochiral C-2 carbon of DEPMPO results in a complex EPR spectrum because of the superimposition of the spectra of two superoxide spin adducts corresponding to the cis and trans adducts, in an ~1:9 ratio (12, 14). Moreover, the 12-line spectrum of the major signal from the *trans*-DEPMPO spin adduct exhibits an alternate line-width phenomenon, which has been attributed to the moderately slow exchange between two conformers ($T_1 \leftrightharpoons T_2$).

To circumvent the alternate line-width effect and the superimposition of the EPR absorptions due to the cis and trans adducts, the *cis*-3-phenyl DEPMPO analogue (DEPMPPOc **5**) was synthesized (17) (Figure 1). Addition of the phenyl group on the C-3 carbon yielded a less complex EPR spectrum (a 12-line spectrum with equal absorption intensity) of the corresponding superoxide adduct (not shown). However, the half-life of this adduct was found to be only 2 min, compared to 17 min for the DEPMPO-OOH adduct (17). 4-PhDEPMPO*c* **6** was synthesized by substituting the phenyl group in the C-4 center (18) (Figure 1). The EPR spectrum of the 4-PhDEPMPO*c*-OOH spin adduct was less complicated, consisting of eight lines. The half-life of this adduct was nearly equal to that of DEPMPO-OOH. Thus, substitution at C-4 by the phosphoryl group results in the generation of a persistent superoxide adduct leading to a much simpler EPR spectrum.

Despite these advances in the chemical synthesis of nitrones, detection of the superoxide adduct in cellular systems still remains a difficult and challenging task. This is mostly due to the rapid reduction of nitroxide spin adducts and to a lack of intracellular targeting and cellular accumulation of nitrone spin traps. With the recent discovery of targeting chemicals conjugated to a triphenylphosphonium group into the mitochondrial compartment, it has become feasible to enhance the intramitochondrial spin trap concentrations (19, 20). To this end, we synthesized a new first generation spin trap, Mito-DEPMPO **7** (21), as shown in Figure 1. In this study, we report the detection, characterization, and kinetics of oxygen-, sulfur-, and carbon-centered radical adducts of Mito-DEPMPO under biologically relevant

[1]Abbreviations: BH_4, tetrahydrobiopterin; BMPO, 5-*tert*-butoxycarbonyl-5-methyl-pyrroline *N*-oxide; DTPA, diethylenetriaminepentaacetic acid; DEPMPPO, 5-(diethoxyphosphoryl)-5-methyl-3-phenyl-pyrroline *N*-oxide; DEPMPO, 5-(diethoxyphosphoryl)-5-methyl-pyrroline *N*-oxide; DMPO, 5,5-dimethyl-pyrroline *N*-oxide; 4-PhDEPMPO*c*, 5-(diethoxyphosphoryl)-5-methyl-4-phenyl-pyrroline *N*-oxide; NHS-DEPMPO, (*N*-hydroxysuccinimidyl-DEPMPO); EMPO, 5-ethoxycarbonyl-5-methyl-pyrroline *N*-oxide; DIBAL-H, diisobutylaluminium hydride; GSNO, *S*-nitrosoglutathione; GPx, glutathione peroxidase; GSH, glutathione reduced; HX, hypoxanthine; nNOS, neuronal nitric oxide synthase; SOD, superoxide dismutase; TEMPO, 2,2,6,6-tetrametylpiperidine-*N*-oxyl; XO, xanthine oxidase.

conditions. Preliminary data indicate the usefulness of Mito-DEPMPO as a viable trap for detecting superoxide generated from intact mitochondria.

Materials and Methods

Chemicals

DEPMPO was obtained from Radical Vision (Marseille, France). (6*R*)-Tetrahydrobiopterin (BH_4), was obtained from Schircks Laboratories (Jona, Switzerland). NADPH, L-arginine, calcium chloride, glutathione (GSH), glutathione oxidase (GPx), xanthine oxidase (XO), hypoxanthine (HX), superoxide dismutase (SOD), catalase, and diethylenetriaminepentaacetic acid (DTPA) were obtained from Sigma Chemical Co. (St. Louis, MO). Calmodulin was obtained from Calbiochem and *S*-nitrosoglutathione (GSNO) from Cayman. Recombinant wild type neuronal nitric oxide synthase (nNOS) was purified in the absence of BH_4 as previously described (22, 23). The spin trap Mito-DEPMPO was also synthesized as previously described (21). Briefly, we used the following procedure.

(i) Synthesis of NHS-DEPMPO—Tributylphosphine (2.16 g, 0.01 mol) was added dropwise to a mixture of diethyl-(1-nitroethan-1-yl)phosphonate (12.58 g, 0.059 mol) and furanone (5 g, 0.059 mol) in cyclohexane (70 mL) and methylene dichloride (CH_2Cl_2) (7 mL) under argon protected from light. The mixture was stirred at room temperature for 66 h. Solvents were distilled under reduced pressure. Purification by flash chromatography on silicagel eluting with a mixture of diethyl ether/pentane (9:1) afforded a yellow oil (14.01 g, 80% yield), corresponding to a mixture of two diastereoisomers of 4-(1-diethoxyphosphoryl-1-nitroethyl)-tetrahydrofuran-2-one. To a solution of 4-(1-diethoxyphosphoryl-1-nitroethyl)-tetrahydrofuran-2-one (1.3 g, 4.4 mmol) in CH_2Cl_2 (35 mL), DIBAL-H (1 M) in hexane (11.45 mL) was added dropwise at −76 °C under dry argon. The reaction mixture was stirred at −78 °C for 3 h, and absolute ethanol (8 mL) was then added at the same temperature. The solution was then filtered on silicagel and dried over Na_2SO_4. After removing the solvent, the expected hemiacetal 4-(1-diethoxyphos-phoryl-1-nitroethyl)-2-hydroxytetrahydrofurane product was isolated by flash chromatography on silicagel eluting with CH_2Cl_2/Et_2O (50: 50) as a pale yellow oil containing four diastereoisomers (714 mg, 55%). To a solution of hemiacetal 4-(1-diethoxyphosphoryl-1-nitroethyl)-2-hydroxytetrahydrofurane (3.8 g, 0.0128 mol) in a mixture of THF/H_2O (10:1) were added NH_4Cl (1.71 g, 0.032 mol) followed by zinc powder (2.09 g, 0.032 mol) at −5 °C over 2 h. The reaction mixture was stirred for 6 h at room temperature in the dark. The precipitate was filtered and washed with CH_2Cl_2 (3 × 40 mL) and MeOH (10 mL). Filtrates were concentrated under reduced pressure, and the residue was dissolved in CH_2Cl_2 (40 mL) and washed with brine (10 mL). The organic layer was dried over Na_2SO_4 and filtered, and the solvent was distilled under reduced pressure. The residual oil was purified by flash chromatography on silicagel (CH_2Cl_2/EtOH, 85:15) to yield two diastereoisomers of the nitrone (2.17 g, 64%). The corresponding *cis*-4-HMDEPMPO (5-diethoxyphosphoryl-5-methyl-4-hydroxymethyl-1-pyrroline *N*-oxide) was obtained as a white solid (1.86 g, 55% yield; mp = 48 °C with decomposition).

To a mixture of *cis*-4-HMDEPMPO (0.18 g, 0.68 mmol) and disuccinimide carbonate (0.209 g, 0.82 mmol) in anhydrous acetonitrile (5 mL) was added triethylamine (0.12 mL, 0.88 mmol) at room temperature under argon. The reaction mixture was stirred for 6 h and then concentrated under reduced pressure. The residue was dissolved in CH_2Cl_2 (10 mL) and washed with saturated $NaHCO_3$ (5 mL) and brine (5 mL) solutions. The organic layer was dried over Na_2SO_4 and the solvent distilled under reduced pressure. Purification of the crude product by flash chromatography on silicagel (CH_2Cl_2/EtOH, 90:10) afforded a white powder (0.26 g, 95%), corresponding to NHS-DEPMPO (5-diethoxyphosphoryl-5-methyl-4-(succinimidyl oxycarbonyloxymethyl)-1-pyrroline *N*-oxide).

(ii) Synthesis of Mito-DEPMPO—To a mixture of NHS-DEPMPO (0.5 g, 1.23 mmol) and (2-aminoethyl) triphenylphos-phonium bromide (0.48 g, 1.24 mmol) in CH_2Cl_2 (30 mL) was added triethylamine (0.23 mL, 1.61 mmol) at room temperature under argon. The reaction mixture was stirred for 2 h and then washed with water (15 mL). The organic layer was dried over Na_2-SO_4 and the solvent distilled under reduced pressure. Purification of the crude product by flash chromatography on silicagel (CH_2-Cl_2/EtOH, 70:30) afforded a white powder (0.57 g, 69%), corresponding to Mito-DEPMPO **7**.

EPR Measurements

EPR spectra were recorded at room temperature or at 37 °C using a Bruker EMX spectrometer at 9.5 GHz (X-band) employing a 100 kHz field modulation. The EPR spectra were simulated using the EPR software developed by A. Rockenbauer from the Chemical Research Center, Budapest, Hungary (24).

(i) Kinetics of the Decay of the Superoxide Spin Adducts—The hypoxanthine/xanthine oxidase (HX/XO) system was used to generate superoxide in phosphate buffer (0.1 M, pH 7.3) at room temperature and at 37 °C, and the superoxide adduct was monitored in the presence of spin trap (20 mM). Once the steady-state levels of the superoxide adduct were reached (approximately 10 min after starting incubation), superoxide adduct formation was terminated using a large excess of SOD (1200 U mL^{-1}), and EPR spectra were recorded at a rate of 1 full scan/2.7 min up to 90 min (32 consecutive spectra). Computer simulations were performed using the ROKI-EPR (24) program. Spectrometer settings were as follows: microwave power, 10 mW; modulation amplitude, 0.63 G; time constant, 0.128 s; gain, 10^5; sweep time, 163 s; and conversion time, 82 ms.

(ii) Kinetics of the Decay of the Mito-DEPMPO-Glutathiyl Adduct—Spectra were obtained by photolysis of a mixture containing GSNO (1 mM), DTPA (1 mM), and Mito-DEPMPO or DEPMPO (20 mM) in phosphate buffer (0.1 M, pH 7.3). The growth of the EPR signal of the Mito-DEPMPO-SG adduct was recorded by positioning on top of the low-field absorption line of the Mito-DEPMPO-SG adduct with the magnetic field turned off. Once the steady-state levels of the Mito-DEPMPO-SG adduct were reached, UV photolysis was terminated and the decay of the spin adduct monitored.

Biochemical Assays

(i) Xanthine Oxidase Activity—The xanthine oxidase activity was determined by monitoring uric acid formation by UV absorption at 260 nm as previously described (25).

(ii) Preparation of Mitochondria—Mitochondria were isolated from RAW 264.7 cells and myocardial tissue as described (26). Briefly, the tissue was homogenized in a H-medium (220 mM mannitol, 70 mM sucrose, 10 mM HEPES at pH 7.0, and 2 mM EDTA) supplemented with protease and phosphatase inhibitors. The homogenate was centrifuged at 2000*g* for 10 min to remove the cellular debris and nuclear pellet. This step was repeated twice to remove the contaminating nuclear fraction. The post-nuclear supernatant was then centrifuged at 10,000*g* for 20 min to pellet out mitochondria. The pellet was washed twice with the H-medium and resuspended in the same buffer. The mitochondrial suspension was layered on sucrose (0.8 M) and centrifuged at 10,000*g* for 20 min to remove any contaminating cytosol and microsomes. The pellet was resuspended in the H-medium, and protein content was estimated by Lowry's method.

(iii) Mitochondrial Oxygen Consumption—Mitochondrial oxygen consumption rates were measured using a Strathkelvin 1302 oxygen electrode with an MT200 Mitocell respiration chamber (Strathkelvin Instruments, Glasgow, U.K.). Measurements were carried out in a final reaction volume of 60 μL. To investigate the effect of spin traps on oxygen consumption, mitochondria (200 μg) were first preincubated with the spin trap at several concentrations for 20 min. At the end of the incubation period, state IV respiration was measured by adding succinate (100 μM). Oxygen consumption was monitored for 10 min and the rate normalized to protein.

Results and Discussion

EPR Characterization of the Mito-DEPMPO-Superoxide Adduct

The Mito-DEPMPO superoxide adduct was obtained using several superoxide ($O_2^{\bullet -}$) generating systems as follows: xanthine/xanthine oxidase, NADPH/neuronal nitric oxide synthase (nNOS), and KO_2 in 18-crown-6 ether. Figure 2a shows the EPR spectrum obtained 10 min after adding XO to a phosphate buffer containing xanthine, Mito-DEPMPO, and DTPA. The computer simulation of the EPR spectrum using the parameters in Table 1 is shown (Figure 2a, bottom). In the presence of superoxide dismutase (SOD), no EPR signal was detected (Figure 2b). In addition, the EPR signal of Mito-DEPMPO-OOH was identical to that obtained from trapping superoxide generated from potassium superoxide (KO_2) in the presence of 18-crown-6 and DMSO (10%) in a phosphate buffer (Supporting Information, Figure 1S). This confirms that the EPR signal shown in Figure 2a is due to the trapping of superoxide. The EPR spectrum of the Mito-DEPMPO-OOH adduct has fewer absorptions as compared to the EPR spectrum of the DEPMPO-OOH adduct (Figure 2c) (14). The computer simulation of the Mito-DEPMPO-OOH adduct revealed only the presence of *trans*-Mito-DEPMPO-OOH.

Superoxide generated by neuronal nitric oxide synthase (nNOS) (27) in the presence of Mito-DEPMPO, calcium, calmodulin, and NADPH yielded the Mito-DEPMPO-OOH

adduct (Figure 3a). The EPR signal of Mito-DEPMPO-OOH decreased when L-arginine was added to the nNOS system (Figure 3b), whereas in the presence of tetrahydrobiopterin (BH_4), Mito-DEPMPO-OOH signal intensity was marginal (Figure 3c). The combination of both L-arginine and BH_4 or the absence of calcium/calmodulin abolished the EPR signal (Figure 3d and e). These results indicate that EPR spin trapping with Mito-DEPMPO is a sensitive method to detect the superoxide formed from neuronal NOS under various conditions.

The EPR spectra (Figures 2a and 3a) of Mito-DEPMPO-OOH can be explained in terms of an exchange model between two conformers of the trans adduct in a chemical equilibrium or by a superimposition model of two different species (hydroxyl and superoxide adducts). The computer simulations of the spectra using the ROKI-EPR program (24) were obtained on the basis of the exchange model (Figure 4a, bottom). As shown in Table 1, the geometry of the Mito-DEPMPO-OOH adduct does not freeze out the chemical exchange between the two conformers of the superoxide spin adduct. First, the increased steric effect of the bulky diethoxyphosphoryl group as compared to that of the methyl group at the position C-5 coupled with the presence of a phosphonium salt group at the C-4 position forces the addition of superoxide to take place on the opposite side of the phosphoryl group. Consequently, *trans*-Mito-DEPMPO-OOH adduct formation is favored (Scheme 1). Second, the alternate line-width phenomenon is less favored with the Mito-DEPMPO-OOH adduct compared to the corresponding DEPMPO-OOH adduct. The exchange rate constants between the respective pairs of conformers are not very different between Mito-DEPMPO-OOH and DEPMPO-OOH adducts ($1.2 \times 10^7\ s^{-1}$ for **7**/$O_2^{\bullet -}$ and $2.9 \times 10^7\ s^{-1}$ for **2**/$O_2^{\bullet -}$).

EPR Characterization of the Mito-DEPMPO-Hydroxyl Adduct

The EPR spectrum of the Mito-DEPMPO-OH adduct, generated using a Fenton system or by reduction of the Mito-DEPMPO-OOH adduct with glutathione peroxidase with glutathione (GPx/GSH), is nearly identical. The EPR spectrum of the Mito-DEPMPO-OH adduct is composed of 12 major absorptions (Figure 4b), compared to the doublet of quartets for the corresponding DEPMPO-OH adduct (14). The EPR signal was totally abrogated upon the addition of catalase to the incubation mixture. The Mito-DEPMPO-OH EPR spectrum was simulated, assuming a predominant contribution from *trans*-Mito-DEPMPO-OH (Figure 4b, bottom).

EPR Characterization of the Mito-DEPMPO-Carbon-Centered and Glutathiyl Adducts

The carbon-centered radicals generated from hydrogen abstraction of the alkyl and acid group via the hydroxyl radical formed from the Fenton system were trapped with Mito-DEPMPO (Supporting Information, Figure 1S). The spectral pattern of Mito-DEPMPO-CH_3(CH)-OH is shown in Figure 5a. The EPR parameters of the carbon-centered adducts are distinctly different from those of the corresponding hydroxyl or superoxide adducts (Table 1).

The Mito-DEPMPO-glutathiyl adduct was generated by photolysing a mixture containing Mito-DEPMPO and GSNO in a phosphate buffer. The EPR spectrum is a doublet of quartets (Figure 5b) with EPR hyperfine parameters a_N and $a_{H\beta}$ very different from corresponding

Mito-DEPMPO-OOH (Table 1). Compared to the DEPMPO-SG adduct, the ratio between the cis and the trans adducts is much smaller for Mito-DEPMPO-SG.

Decay Kinetics of Mito-DEPMPO-OOH and Mito-DEP-MPO-SG Adducts

The kinetics of decay of the superoxide radical adduct was determined by adding a large amount of SOD (1200 U mL^{-1}) to the incubation of HX/XO with DEPMPO or Mito-DEPMPO, after adduct formation reached a steady-state concentration. Because the EPR spectra of the DEPMPO-OOH and DEPMPO-OH adducts do not overlap, the decay of DEPMPO-OOH could be conveniently monitored. In contrast, the EPR spectrum of the Mito-DEPMPO-OOH adduct overlaps considerably with the EPR spectrum of the Mito-DEPMPO-OH, making it very difficult to determine the kinetics of radical adducts. Thus, the decay of the Mito-DEPMPO-OOH was calculated using the ROKI-EPR program (24). With this program, it was feasible to determine the concomitant evolution of different radical adducts (as described below). The kinetics of decay of the Mito-DEPMPO-OOH and DEPMPO-OOH adducts were tested in parallel under the same set of conditions. Solutions containing hypoxanthine (0.4 mM), xanthine oxidase (0.04 U mL^{-1}), DTPA (1 mM), and Mito-DEPMPO or DEPMPO (20 mM) in a phosphate buffer (0.1 M, pH 7.3) were incubated at room temperature or at 37 °C. Once the adduct concentration had reached a steady-state (in approximately 9 min), a large amount of SOD (1200 U mL^{-1}) was added, and each spectrum was subsequently recorded within 90 min at a rate of 1 full scan/2.7 min (Figure 6 and Supporting Information, Figures 2S and 3S).

The ROKI-EPR program was first used to simulate the pure spectra of the adduct (hydroxyl and superoxide) in the conventional fashion. The 32 consecutive spectra were then simulated by using fixed EPR parameters, with only the amplitudes modulated by a kinetic function describing a mixed first- and second-order decay process. The absolute radical concentration was determined by simulation, comparing the signal intensity of Mito-DEPMPO-OH and Mito-DEPMPO-OOH adducts with that of the TEMPO (0.01 mM) solution. The computations showed that the half-life times for Mito-DEPMPO-OOH were 40.4 and 17.3 min at room temperature and 37 °C, respectively. In contrast, the DEPMPO-OOH adduct decayed over 15.3 min (at room temperature) and 8.7 min at 37 °C (Figure 6c, Table 2, and Supporting Information, Figure 4S).

The increased persistence of Mito-DEPMPO-OOH compared to that of DEPMPO-OOH may be attributed to the steric hindrance caused by the presence of the phosphonium group. The addition of the superoxide anion on the side opposite to that of the phosphoryl group results in the conformation of a nitroxide in which the HOO- and phosphoryl groups are in a pseudoaxial position, probably resulting in its stabilization through anomeric or hyperconjugative mechanism. The efficient trapping of superoxide by Mito-DEPMPO (Table 2) may also be explained by the presence of the cationic group, increasing the electrostatic attraction for the superoxide anion.

Glutathiyl radicals were continuously generated by the photolysis (170 W) of GSNO (1 mM). In the presence of Mito-DEPMPO (20 mM) or DEPMPO (20 mM) in phosphate buffer (0.1 M, pH 7.3), the corresponding radical adduct attributable to Mito-DEPMPO-SG was obtained. Photolysis was terminated once the concentration of the adduct reached a

maximal value (Figure 7), and the rate of Mito-DEPMPO-SG or DEPMPO-SG was followed for the next 70 min at a rate of 1 full scan/2.7 min (Figure 7 and Supporting Information, Figure 6S). From the kinetic parameters, the half-life of the Mito-DEPMPO-SG adduct was estimated to be greater than that of the DEPMPO-SG adduct (Table 2). This property makes Mito-DEPMPO a more versatile spin trap for biological applications.

Trapping of ROS Formed from Isolated Mitochondria by DEPMPO and Mito-DEPMPO

Experiments were performed with mitochondria isolated from RAW 264.7 cells. Addition of succinate to an incubation mixture containing mitochondria and Mito-DEPMPO in phosphate buffer yielded an EPR spectrum consisting of a mixture of superoxide (41%), hydroxyl (38%), and alkyl adducts (21%) (Figure 8a). In contrast, little or no superoxide adduct was detected with DEPMPO; only a weak signal from the hydroxyl adduct was observed (Figure 8e). In the absence of succinate, the EPR spectrum of Mito-DEPMPO-OOH was less intense (Figure 8b). These results indicate that Mito-DEPMPO, not DEPMPO, generates detectable superoxide adduct from intact mitochondria. The EPR spectrum of the Mito-DEPMPO-OOH adduct was greatly inhibited in the presence of argon (Figure 8c). Oxygen consumption measurements showed that Mito-DEPMPO did not significantly affect mitochondrial respiration (Supporting Information, Table 1S). In the absence of mitochondria, no EPR signal was observed from incubations containing spin trap and succinate at 37 °C (Figure 8d and h). Figure 9 shows the effect of SOD on Mito-DEPMPO and DEPMPO spin adducts formed from succinate-induced mitochondrial oxygen consumption. The Mito-DEPMPO-OOH adduct formed from intact mitochondria was partially inhibited by SOD (150 U mL^{-1}) (Figure 9a and b). However, SOD completely abrogated the Mito-DEPMPO-OOH and DEPMPO-OOH adducts formed from permeabilized mitochondria. Clearly, these results suggest that Mito-DEPMPO-OOH was primarily formed from the trapping of extramitochondrial superoxide but not intra-mitochondrial superoxide. Additional experiments using other Mito-DEPMPO analogues are needed to fully resolve this problem.

Conclusions

Superoxide reaction with Mito-DEPMPO is stereoselective forming the trans isomer as the only one major product. The EPR spectrum of the Mito-DEPMPO-OOH spin adduct is simpler than that of the DEPMPO-OOH. In addition, the Mito-DEPMPO-superoxide spin adduct is more persistent than the DEPMPO-OOH adduct. The Mito-DEPMPO-glutathiyl spin adduct is also more persistent than the corresponding DEPMPO-glutathiyl adduct. Thus, Mito-DEPMPO is a more versatile spin trap for detecting superoxide and thiyl radicals generated in biological systems.

Supplementary Material

Refer to Web version on PubMed Central for supplementary material.

Acknowledgments

A.R. thanks the Hungarian Science Fund for partial funding of this work (grant OTKA T-046953). This work was supported by National Institutes of Health Grants (HL07305-1 to B.K. and HL67244 to J.V.-V.).

References

1. Chalfont GR, Perkins MJ, Horsfield A. Probe for homolytic reactions in solution. II Polymerization of styrene. J Am Chem Soc. 1968; 90:7141–7142.
2. Janzen EG, Blackburn B. Detection and identification of short-lived free radicals by an electron spin resonance trapping technique. J Am Chem Soc. 1968; 90:5909–5910.
3. Hata Y, Watanabe M, Tonda K, Hirata M. Aziridine biotransformation by microsomes and lethality to hepatocytes isolated from rat. Chem-Biol Interact. 1987; 63:171–184. [PubMed: 3664792]
4. Hampton MJ, Floyd RA, Janzen EG, Shetty RV. Mutagenicity of free-radical spin-trapping compounds. Mutat Res. 1981; 91:279–283. [PubMed: 7022198]
5. Hideg E, Takàtsy A, Sar CP, Vass I, Hideg K. Utilizing new adamantyl spin traps in studying UV-B-induced oxidative damage of photosystem II. J Photochem Photobiol, B. 1999; 48:174–179.
6. Ho WF, Gilbert BC, Davies MJ. EPR spin-trapping studies of radicals generated from the Fe^{II}-catalysed degradation of nucleobase, nucleoside, RNA and DNA hydroperoxides. J Chem Soc, Perkin Trans. 1997; 2:2525–2531.
7. Mason RP, Hanna PM, Burkitt MJ, Kadiiska MB. Detection of oxygen-derived radicals in biological systems using electron spin resonance. Environ Health Perspect Suppl. 1994; 102:33–36.
8. Khan N, Wilmot CM, Rosen GM, Demidenko E, Sun J, Joseph J, O'Hara J, Kalyanaraman B, Swartz HM. Spin traps: in vitro toxicity and stability of radical adducts. Free Radical Biol Med. 2003; 34:1473–1481. [PubMed: 12757857]
9. Finkelstein E, Rosen GM, Rauckman EJ. Spin trapping. Kinetics of the reaction of superoxide and hydroxyl radicals with nitrones. J Am Chem Soc. 1980; 102:4994–4999.
10. Halliwell, B.; Gutteridge, JM. Free Radicals in Biology and Medicine. Oxford University Press; Oxford, U.K: 1999.
11. Karoui H, Clement JL, Rockenbauer A, Siri D, Tordo P. Synthesis and structure of 5,5-diethoxycarbonyl-1-pyrroline *N*-oxide (DECPO). Application to superoxide radical trapping. Tetrahedron Lett. 2004; 45:149–152.
12. Fréjaville C, Karoui H, Tuccio B, Le Moigne F, Culcasi M, Pietri S, Lauricella R, Tordo P. 5-Diethoxyphosphoryl-5-methyl-1-pyrroline *N*-oxide (DEPMPO): a new phosphorylated nitrone for the efficient *in vitro* and *in vivo* spin trapping of oxygen-centred radicals. J Chem Soc, Chem Commun. 1994; 15:1793–1794.
13. Olive G, Mercier A, Le Moigne F, Rockenbauer A, Tordo P. 2-Ethoxycarbonyl-2-methyl-3,4-dihydro-2*H*-pyrrole-1-oxide: evaluation of the spin trapping properties. Free Radical Biol Med. 2000; 28:403–408. [PubMed: 10699752]
14. Frejaville C, Karoui H, Tuccio B, Le Moigne F, Culcasi M, Pietri S, Lauricella R, Tordo P. 5-(Diethoxyphosphoryl)-5-methyl-1-pyrroline N-oxide: a new efficient phosphorylated nitrone for the in vitro and in vivo spin trapping of oxygen-centered radicals. J Med Chem. 1995; 38:258–265. [PubMed: 7830268]
15. Villamena FA, Zweier JL. Superoxide radical trapping and spin adduct decay of 5-*tert*-butoxycarbonyl-5-methyl-1-pyrroline *N*-oxide (BocMPO): kinetics and theoretical analysis. J Chem Soc, Perkin Trans. 2002; 2:1340–1344.
16. Zhao H, Joseph J, Zhang H, Karoui H, Kalyanaraman B. synthesis and biochemical applications of a solid cyclic nitrone spin trap: a relatively superior trap for detecting superoxide anions and glutathiyl radicals. Free Radical Biol Med. 2001; 31:599–606. [PubMed: 11522444]
17. Nsanzumuhire C, Clément JL, Ouari O, Karoui H, Finet JP, Tordo P. Synthesis of the *cis* diastereoisomer of 5-di-ethoxyphosphoryl-5-methyl-3-phenyl-1-pyrroline *N*-oxide (DEPMP-PO*c*) and ESR study of its superoxide spin adduct. Tetrahedron Lett. 2004; 45:6385–6389.
18. Hardy M, Chalier F, Finet JP, Rockenbauer A, Tordo P. Diastereoselective synthesis and ESR study of 4-phenylDEP-MPO spin traps. J Org Chem. 2005; 70:2135–2142. [PubMed: 15760197]
19. Coulter CV, Kelso GF, Lin TK, Smith RAJ, Murphy MP. Mitochondrially targeted antioxidants and thiol reagents. Free Radical Biol Med. 2000; 28:1547–1554. [PubMed: 10927180]
20. Dhanasekaran A, Kotamraju S, Karunakaran C, Kalivendi SV, Thomas S, Joseph J, Kalyanaraman B. Mitochondria superoxide dismutase mimetic inhibits peroxide-induced oxidative damage and

apoptosis: role of mitochondrial superoxide. Free Radical Biol Med. 2005; 39:567–583. [PubMed: 16085176]

21. Hardy M, Chalier F, Ouari O, Finet JP, Rockenbauer A, Kalyanaraman B, Tordo P. Mito-DEPMPO synthesized from a novel NH2-reactive DEPMPO spin trap: a new and improved trap for the detection of superoxide. Chem Commun. 2007; 10:1083–1085.
22. Martasek P, Miller RT, Liu Q, Roman LJ, Salerno JC, Migita CT, Raman CS, Gross SS, Ikeda-Saito M, Masters BSS. The C331A mutant of neuronal nitric-oxide synthase is defective in arginine binding. J Biol Chem. 1998; 273:34799–34805. [PubMed: 9857005]
23. Roman LJ, Sheta EA, Martasek P, Gross SS, Liu Q, Masters BSS. High-level expression of functional rat neuronal nitric oxide synthase in *Escherichia coli*. Proc Natl Acad Sci USA. 1995; 92:8428–8432. [PubMed: 7545302]
24. Rockenbauer A, Korecz L. Automatic computer simulations of ESR spectra. Appl Magn Reson. 1996; 10:29–43.
25. Wede I, Altindag ZZ, Widner B, Wachter H, Fuchs D. Inhibition of xanthine oxidase by pterins. Free Radical Res. 1998; 29:331–338. [PubMed: 9860048]
26. Prabu SK, Anandatheerthavarada HK, Raza H, Srinivasan S, Spear JF, Avadhani NG. Protein kinase A-mediated phosphorylation modulates cytochrome c oxidase function and augments hypoxia and myocardial ischemia-related injury. J Biol Chem. 2006; 281:2061–2070. [PubMed: 16303765]
27. Vasquez-Vivar J, Hogg N, Martasek P, Karoui H, Pritchard JKA, Kalyanaraman B. Tetrahydrobiopterin-dependent inhibition of superoxide generation from neuronal nitric oxide synthase. J Biol Chem. 1999; 274:26736–26742. [PubMed: 10480877]

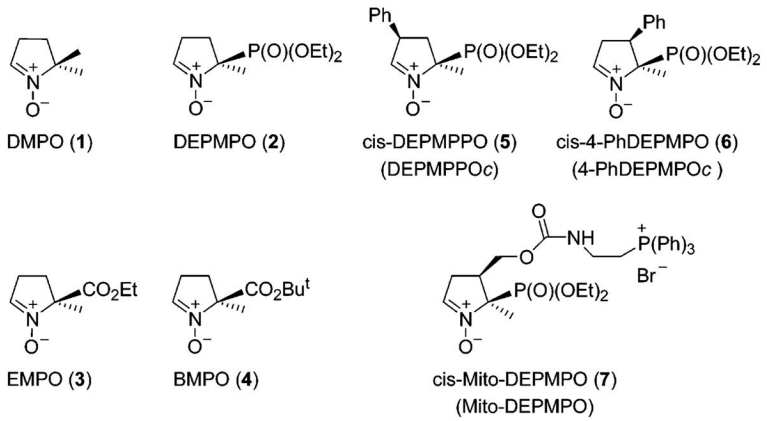

Figure 1.
Chemical structures of the cyclic nitrones.

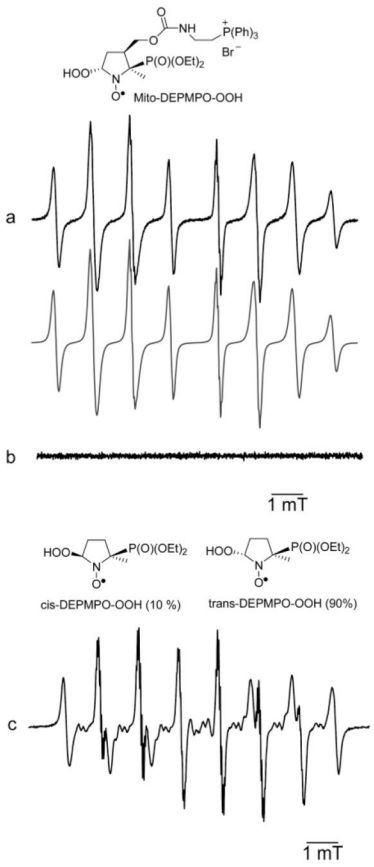

Figure 2.

Spin trapping of superoxide with Mito-DEPMPO. (a) EPR spectrum obtained after 10 min of incubation of a mixture containing hypoxanthine (HX) (0.4 mM), xanthine oxidase (XO) (0.04 U mL^{-1}), DTPA (1 mM), and Mito-DEPMPO (20 mM) in a phosphate buffer (0.1 M, pH 7.3), (b) The same as that in (a) but in the presence of SOD (1200 U mL^{-1}). (c) The same as that in (a) but containing DEPMPO. The gray line represents the computer simulation of the spectrum with parameters given in Table 1. Spectrometer settings: microwave power, 10 mW (a–c); modulation amplitude, 0.2 G (a–c); time constant, 0.640 ms (a–c); gain, 10^5 (a–c); sweep time, 671.77 s (a–c); and conversion time, 327.68 ms (a–c).

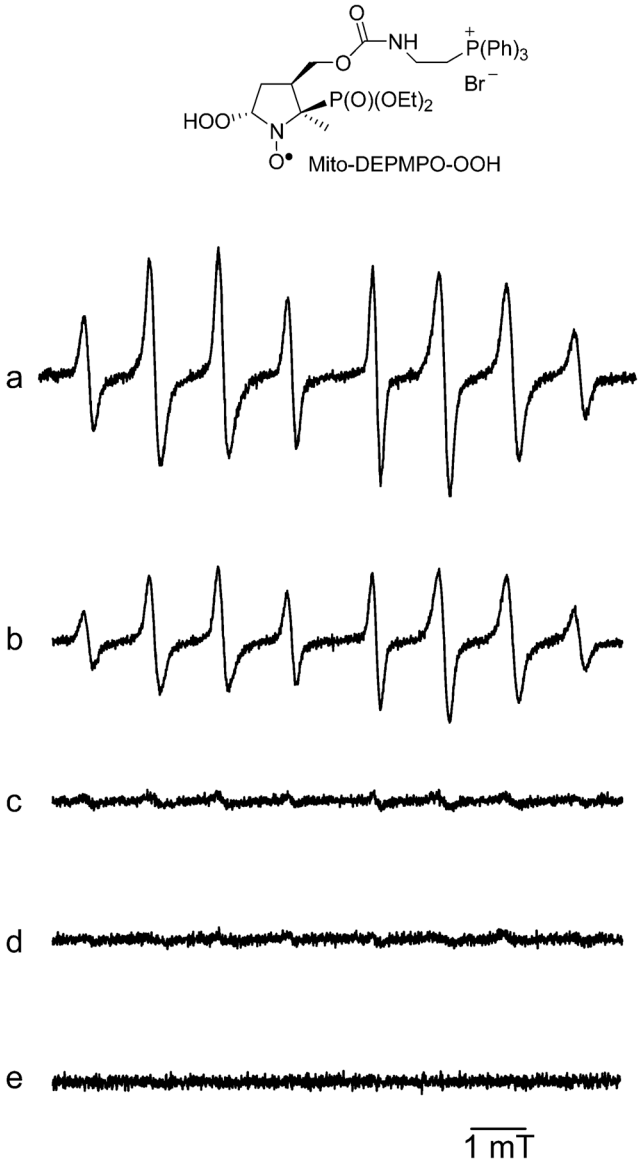

Figure 3.

Detection of superoxide from nNOS with Mito-DEPMPO. (a) EPR spectrum obtained after 4 min of incubation of a mixture containing neuronal nitric oxide synthase (nNOS) (1.4 μg), calcium (0.2 mM), calmodulin (20 μg/mL), Mito-DEPMPO (20 mM), and NADPH (0.1 mM) in HEPES buffer (50 mM, pH 7.4) containing 0.1 mM DTPA. (b) The same as that in (a) but with L-arginine (1 mM). (c) The same as that in (a) but with tetrahydrobiopterin (BH_4) (10 μM). (d) The same as that in (a) but in the presence of L-arginine (1 mM) and BH_4 (10 μM). (e) The same as that in (a) but in the absence of calcium/calmodulin. Spectrometer settings: microwave power, 10 mW (a–e); modulation amplitude, 0.63 G (a–e); time constant, 1.28 ms (a–e); gain, 10^5 (a–e); sweep time, 167.77 s (a–e); and conversion time, 0.082 s (a–e).

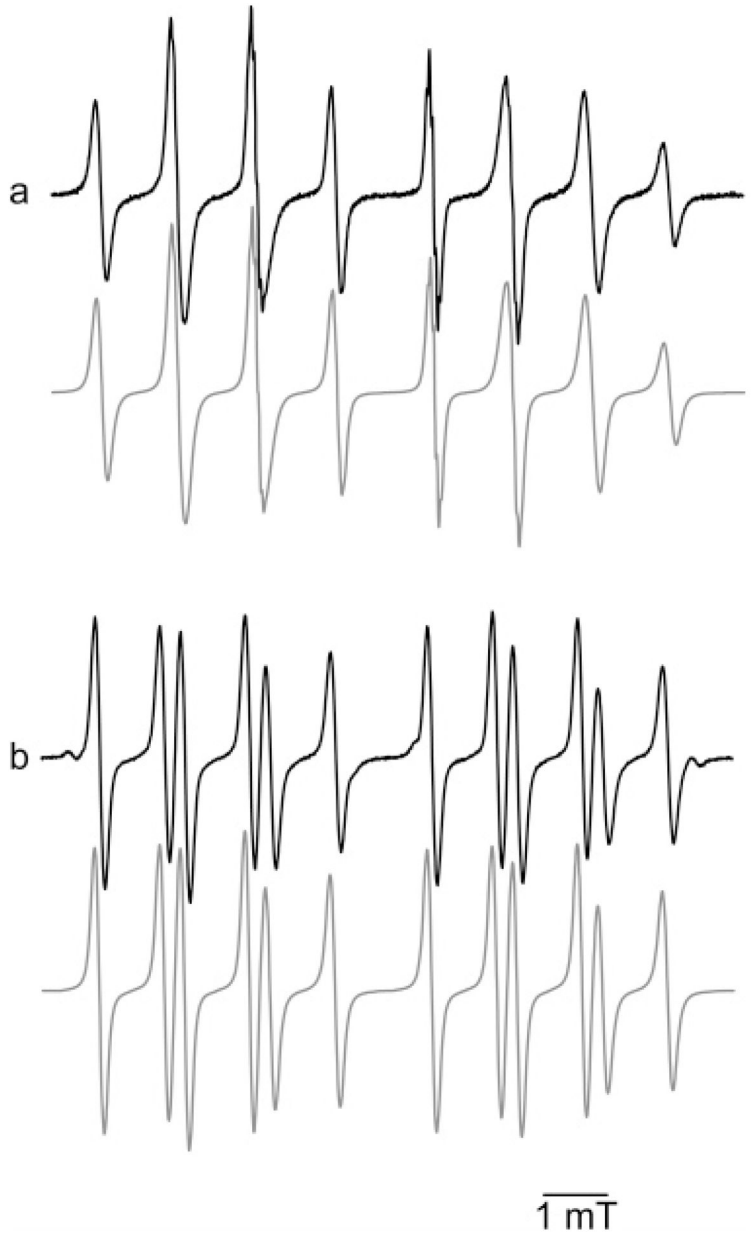

Figure 4.

Spin trapping of hydroxyl radical with Mito-DEPMPO. (a) EPR spectrum obtained after 10 min of incubation of a mixture containing hypoxanthine (HX) (0.4 mM), xanthine oxidase (XO) (0.04 U mL^{-1}), DTPA (1 mM), and Mito-DEPMPO (20 mM) in a phosphate buffer (0.1 M, pH 7.3). (b) Spectrum obtained 10 min after the reduction of the respective superoxide adduct obtained in (a) by adding GPx (10 U mL^{-1}) and GSH (1.2 mM) to the mixture followed by 2 min of bubbling argon gas. The gray line represents the computer simulation of the spectra with the parameters given in Table 1. Spectrometer settings: microwave power, 10 mW, (a) and 20 mW (b); modulation amplitude, 0.2 (a) and 0.8 G (b); time constant, 0.640 ms (a) and 1.28 ms (b); gain, 10^5 (a and b); sweep time, 671.77 s (a) and 167.77 s (b); and conversion time, 327.68 ms (a) and 82 ms (b).

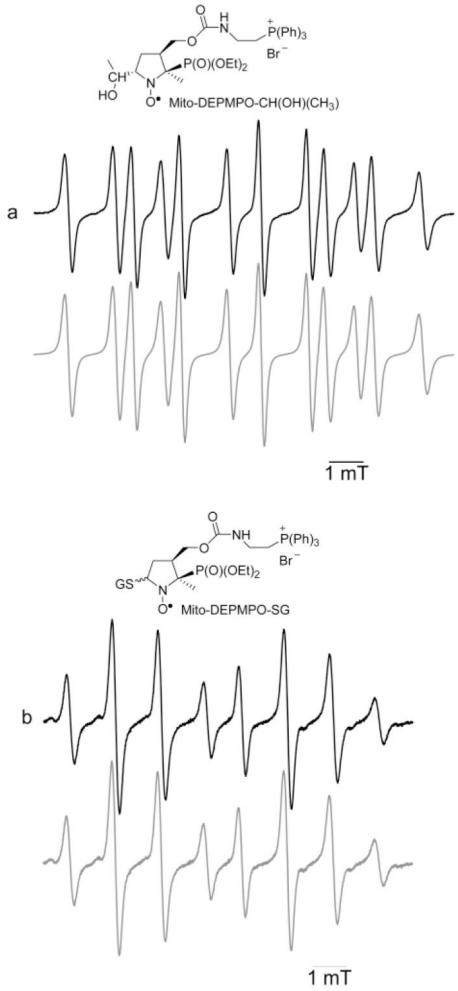

Figure 5.

Spin trapping of an α-hydroxyethyl carbon centered radical and a glutathiyl radical with Mito-DEPMPO. (a) EPR spectrum obtained after 30 min of incubation of a mixture containing Mito-DEPMPO (20 mM), H_2O_2 (2 mM), $FeSO_4$ (2 mM), DTPA (1 mM), and EtOH (5%) in phosphate buffer (0.1 M, pH 7.3). (b) Spectrum obtained after 10 min of photolysis of a mixture containing Mito-DEPMPO (20 mM), GSNO (1 mM), DTPA (1 mM). and phosphate buffer (0.1 M, pH 7.3). The gray line represents the computer simulation of the spectra with the parameters given in Table 1. Spectrometer settings: microwave power, 10 mW (a and b); modulation amplitude, 0.5 G (a) and 0.63 G (b); time constant, 0.640 ms (a) and 1.28 ms (b); gain, 10^5 (a and b); sweep time, 335.54 s (a and b); and conversion time, 0.163 s (a and b).

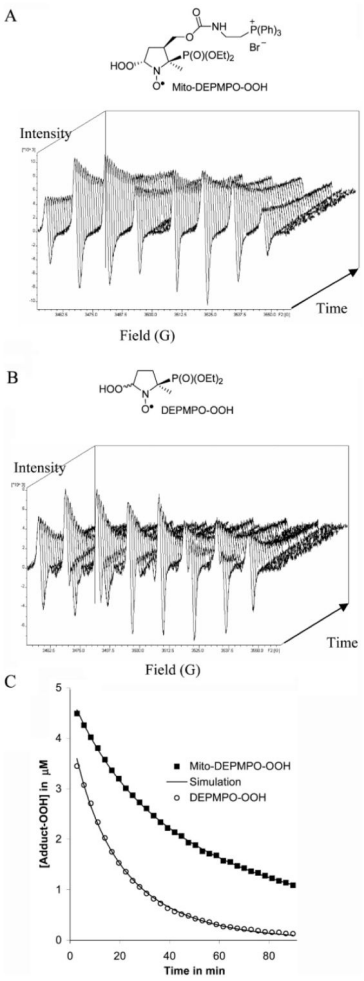

Figure 6.

Kinetics of the decay of the Mito-DEPMPO-OOH and the DEPMPO-OOH at room temperature. (A) Kinetics of the decay of the Mito-DEPMPO-OOH superoxide adduct. (B) Kinetics of the decay of the DEPMPO-OOH superoxide adduct. (C) Decay curves for the Mito-DEPMPO-OOH and DEPMPO-OOH adducts. The gray line was computed by a combination of first- and second-order kinetics. The symbols (■) and (○) represent the 32 experimental spectra of Mito-DEPMPO-OOH and DEPMPO-OOH, respectively.

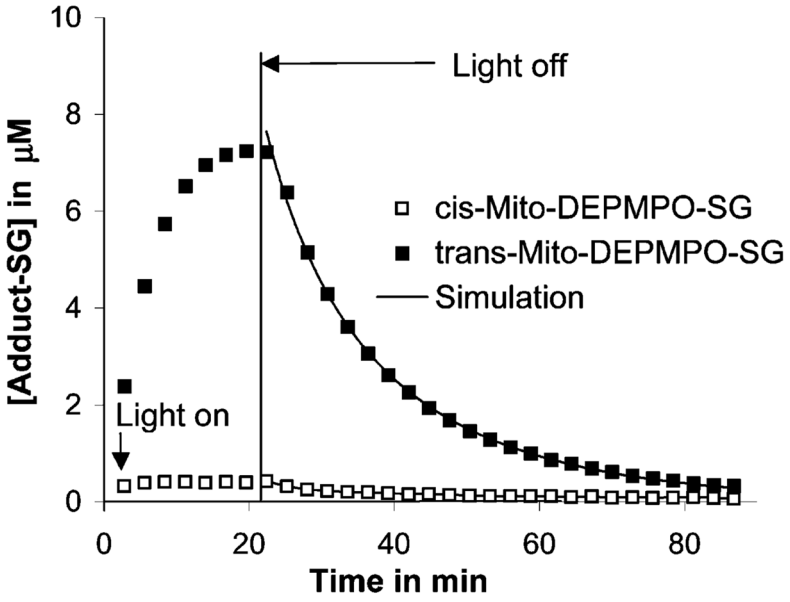

Figure 7.

Kinetics of the decay of the Mito-DEPMPO-SG adduct. The time-dependent growth and decay of the of Mito-DEPMPO-SG adduct generated by photolysis of GSNO is shown. The gray line indicates the concentration calculated by the mixed decay model. The symbols (■) and (○) represent the experimental spectra of *trans*-Mito-DEPMPO-SG and *cis*-Mito-DEPMPO-SG, respectively.

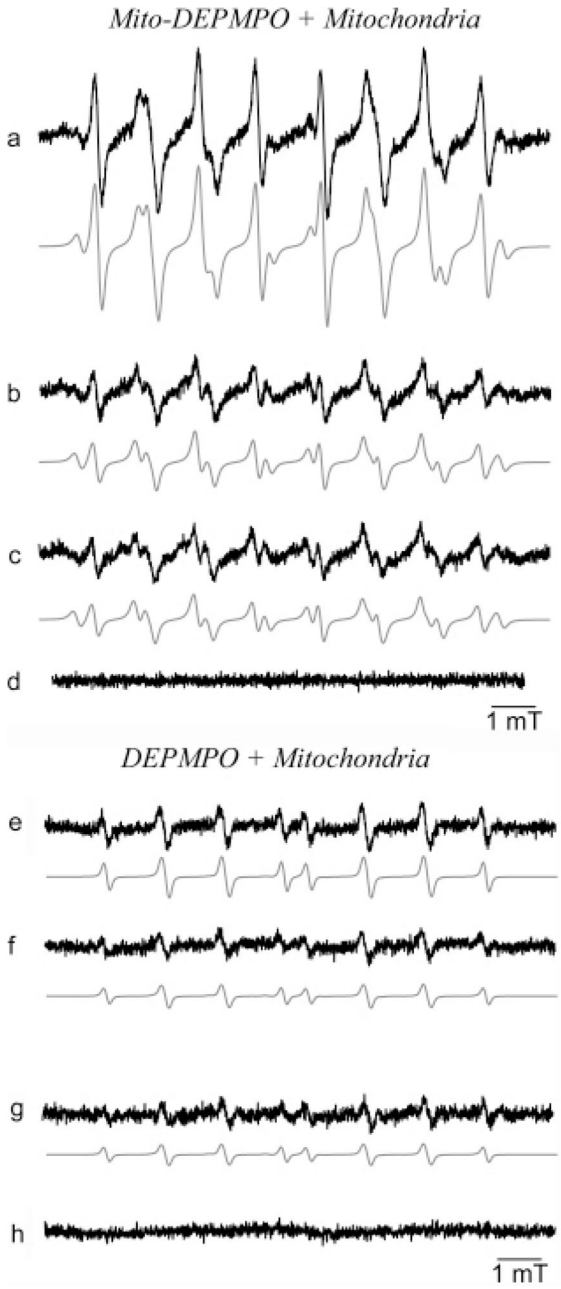

Figure 8.

Spin trapping of the reactive oxygen species formed from isolated mitochondria. (a) EPR spectrum obtained from isolated mitochondria following stimulation with succinate. Mitochondria (200 μg) were incubated with Mito-DEPMPO (50 mM) in a phosphate buffer at pH 7.3 for 20 min, and succinate (100 μM) was added to this mixture at 37 °C; (b) the same as that in (a) but without succinate; (c) the same as that in (a) but with argon (bubbling for 30 s); (d) the same as that in (a) but without mitochondria; (e) the same as that in (a) but with DEPMPO (50 mM); (f) the same as that in (b) but with DEPMPO (50 mM); (g) the same as that in (c) but with DEPMPO (50 mM); and (h) the same as that in (d) but with

DEPMPO (50 mM). The gray line represents the computer simulation of the spectra. Spectrometer settings: microwave power, 20 mW (a–h); modulation amplitude, 1 G (a–h); time constant, 1.28 ms (a–h); gain, 10^6 (a–h); sweep time, 335.54 s (a–h); conversion time, 0.163 s (a–h), 3 scans (a–h).

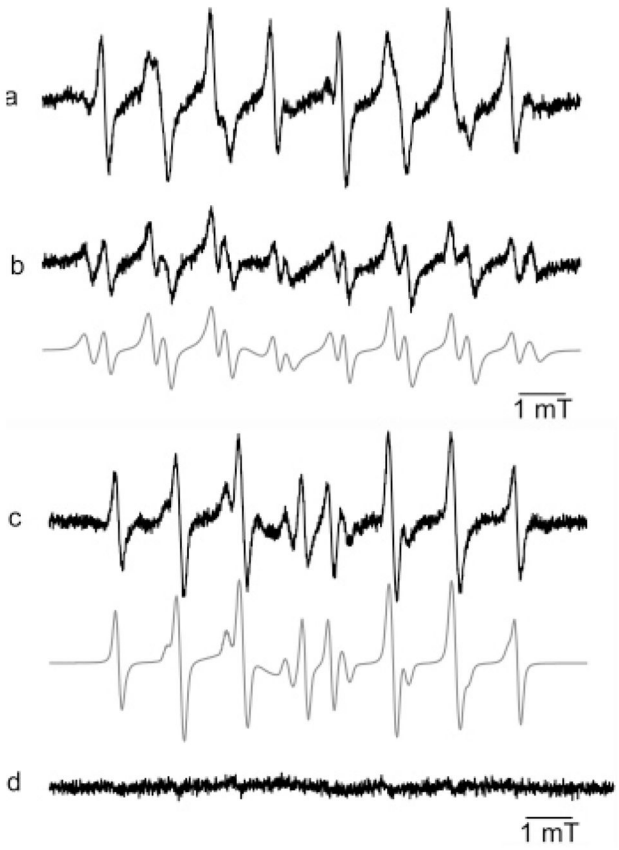

Figure 9.

Effect of SOD on Mito-DEPMPO and DEPMPO oxy radical adducts. (a) Signal obtained in the presence of isolated mitochondria (200 μg) with Mito-DEPMPO (50 mM) in phosphate buffer at pH 7.3 after 20 min of incubation with the subsequent addition of succinate (100 μM) at 37 °C. (b) The same as that in (a) but with SOD (100 U mL^{-1}). (c) Signal obtained in the presence of permeabilized mitochondria (200 μg) in the presence of lauryl maltoside (8 mM) with DEPMPO (50 mM) in phosphate buffer at pH 7.3 after adding succinate (100 μM) at 37 °C. (d) The same as that in (c) but with SOD (100 U mL^{-1}). The gray line represents the computer simulation of the spectra. Spectrometer settings: microwave power, 20 mW (a–d); modulation amplitude, 1 G (a–d); time constant, 1.28 ms (a–d); gain 10^6 (a–d); sweep time, 335.54 s (a–d); conversion time, 0.163 s (a–d), 3 scans (a–d).

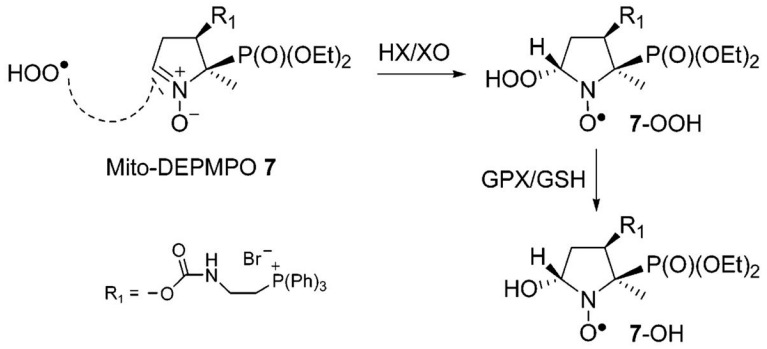

Scheme 1.
Stereoselectivity Formation of 7-OH

Table 1

EPR Parameters of Mito-DEPMPO Spin Adducts

spin adduct	generating system	diastereoisomer	conformer	k (s^{-1})[a]	a_P (G)	a_N (G)	$a_{H\beta}$ (G)	$a_{H\gamma}$ (G)[b]
7-OOH	HX/XO; nNOS; KO_2 System	*trans* (100%)	T_1 (69.7%)	0.12×10^8	53.27	12.79	12.37	0.5 (3), 0.48 (2), 0.44, 0.16
			T_2 (30.3%)		52.01	12.97	10.13	
7-OH	GPx/GSH				52.90	12.97	10.34	
7-SG	GSNO (1 mM), hν	*trans* (77.4%)			51.22	13.77	13.24	
		cis (22.6%)			55.83	13.93	17.94	
7-Me	Fe^{++}, H_2O_2, DMSO (10%)				57.10	14.73	18.08	
7-CH_2OH	Fe^{++}, H_2O_2, MeOH (7%)				57.53	14.32	19.12	
7-$CH(OH)CH_3$	Fe^{++}, H_2O_2, EtOH (5%)				57.55	14.32	19.50	
7-COOH	Fe^{++}, H_2O_2, HCOOH (7%)				53.82	13.95	15.96	

[a] Exchange rate constants are in s^{-1}.

[b] The number of equivalent protons is given in parenthesis.

Table 2

Kinetic Parameters of Spin Adducts

	7-OOH (rt)	2-OOH (rt)	7-OOH (37 °C)	2-OOH (37 °C)	7-SG (rt)	2-SG (rt)
k_1/min^{-1}	0.00915	0.0366	0.0337	0.0615	0.042	0.120
k_2/min^{-1}mM^{-1}	1.64	2.97	1.84	8.84	2.4	11.1
[cc]$_0$/μMol	4.50	3.45	3.96	2.52		
$t_{1/2}$ app/min[a]	40.4	15.3	17.3	8.7	12.2	4.6

[a] $t_{1/2}$ app is the apparent half-life time in the experiment, rt is the room temperature, and [cc]$_0$ is the initial concentration.